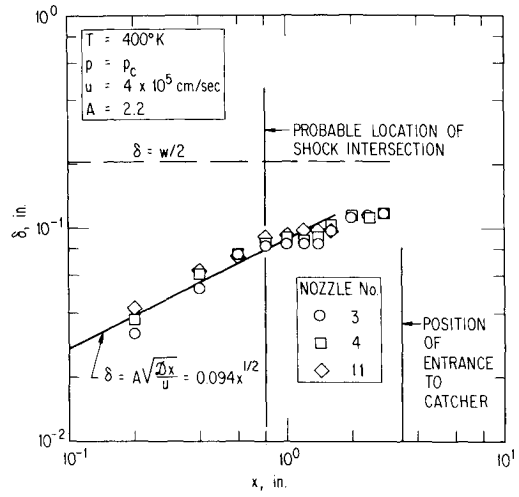

Fig. 4 Position of luminous front in primary nozzle flow for cavity pressure equal to nozzle exit static pressure with secondary flow of 1 g/sec each He and H_2 injected.

from the nozzle width w, and the difference was divided by two as indicated in Fig. 3.

For tests in which there was no flow in the secondary nozzles, the rate of growth of the reaction zone appeared to be linear. When the exit pressures in the primary and tertiary nozzles were equal [Fig. 2a] the constant of proportionality $\bar{A}$ was approximately 0.09 (Fig. 3, solid curve), which is remarkably close to the nominal value for turbulent mixing.[6] When the ambient cavity pressure was larger than the nozzle exit freestream pressure [Fig. 2b], the growth of the reaction zone was steeper as shown in Fig. 3 by the dashed line curve, which represents a linear least squares fit to the data. The shock waves can be estimated from Figs 2a and 2b as previously noted, and the difference in flow deflection angle obtained. By subtracting the difference in turning angle from the regression line of the data for Fig. 2b and translating the line to account for the shock wave originating further upstream, we obtained a curve that fell within the scatter of the data from Fig. 2a ($p = p_c$). Although the line does not have the same slope as the linear regression line fitted to these data, it is closer to that slope (0.11 corrected from 0.14 compared to 0.09) than the value uncorrected for turning angle difference. Apparently, the larger angle of growth of the reaction zone associated with flows with high ambient pressure relative to nozzle exit static pressure is closely related to the strength of the shock wave associated with the flow.

When a secondary flow consisting of half He and half H_2 was introduced and the exit pressures were matched, the growth of luminous front appeared to be proportional to $x^{1/2}$ (Fig. 4), i.e., laminar according to Eq. (1). Computation of A from these measurements yields either 4.7 or 2.2, depending on whether D/u is evaluated on the basis of conditions at the nozzle exit or those more characteristic of the cavity further downstream. Conditions further downstream were taken from Ref. 7. These are $T = 400$ K, $p = p_c$, the downstream cavity pressure, and $u = 3 \times 10^5$ cm/sec.

Thus, both laminar and turbulent mixing characteristics have been observed. The presence of laminar mixing appears to require matched exit pressures and the absence of a significant base region, i.e., when there was no flow in the secondary nozzles, these nozzles correspond to a base region between the primary and tertiary nozzles.

Whether emission from the visible overtones in these observations actually represents the leading edge of the mixing and reacting gas layers is not clearly evident. To examine this question a spectrographic measurement was made. The $P_1{}^6$ line of the P rotational branch of the 1 to 0 vibrational transition of the HF molecule at 2.708 μ was observed for flow conditions similar to those of Test 3 of Fig. 3. From these observations a spreading rate of the mixing and reacting flow can be obtained from which an equivalent to the luminous front position of the photographic observations can be determined. When such data were plotted on Fig. 3 they appeared to fall within the scatter of the data obtained from the photographic observations for Test 3 conditions. Consequently, one would conclude that the photographic method can provide measurements that well represent the location of the mixing and reacting front.

Since this study was completed, the work of Shackleford et al.[8] has been reported. These mixing studies used two large-scale nozzles. Mixing was between parallel flows of reactant gases, and the diluent gas was N_2 rather than He. Also, nozzle geometry differed significantly, e.g., Shackleford has no base region between nozzles, making comparison between the two studies difficult. Both Shackleford's studies and this one isolated conditions of laminar and turbulent mixing: the studies of Ref. 8 examined the effect of the Reynolds number, while the present study effectively varied mixing geometry. Nevertheless, for laminar mixing both works showed reaction layer growth proportional to $x^{1/2}$, and for turbulent flows agreement for the value $\bar{A}$ is good (0.09 compared with 0.08).

References

[1] Varwig, R. L., "Photographic Observations of CW HF Chemical Laser Reacting Flow Field," TR-0073(3250-10)-8, Nov. 1972, The Aerospace Corp., El Segundo, Calif.

[2] Durran, D. A. and Varwig, R. L., "Performance of Triple Slit Nozzle for Chemical Laser Applications," TR-0073(3240-10)-3, Oct. 1972, The Aerospace Corp., El Segundo, Calif.

[3] Warren, W. R., Jr., "Reacting Flow and Pressure Recovery Processes in HF/DF Chemical Lasers," presented at 4th International Colloquium on Gas Dynamics of Explosions and Reactive Systems, Univ. of California at San Diego, July 10–13, 1973.

[4] Ellinwood, J. W. and Mirels, H., "Laminar Flamesheet With Hypersonic Viscous Interaction," *AIAA Journal*, Vol. 10, No. 6, June 1972, pp. 830–832.

[5] Mirels, H., Hofland, R., and King, W. S., "Simplified Model of CW Diffusion-Type Chemical Laser," *AIAA Journal*, Vol. 11, No. 2, Feb. 1973, pp. 156–164.

[6] Schlichting, H., *Boundary Layer Theory*, 4th ed., McGraw-Hill, New York, 1960, pp. 598–600.

[7] Varwig, R. L. and Kwok, M. A., "CW HF Chemical Laser Flow Diagnostic Measurements," *AIAA Journal*, Vol. 12, No. 2, Feb. 1974, pp. 208–212.

[8] Shackleford, W. L., Witte, A. B., Broadwell, J. E., Trost, J. E., Jacobs, T. A., "Experimental Studies of Chemically Reactive ($F+H_2$) Flow in Supersonic Free Jet Mixing Layers," *AIAA Journal*, Vol. 12, No. 8, Aug. 1974, pp. 1009–1010.

Improved Approximation of Constitutive Elasto-Plastic Stress-Strain Relationship for Finite Element Analysis

T. R. Hsu* and A. W. M. Bertels†
University of Manitoba, Winnipeg, Canada

With the increasing demand of nuclear power and aerospace applications, the elasto-plastic stress analysis of solid structures has become absolutely necessary. Finite element analysis has shown to be one of the most promising and practical methods for these applications as illustrated in Ref. 1.

Since the relationship of stress vs strain is nonlinear for material undergoing plastic deformation, constant change of the

Received May 3, 1974.
Index categories: Aircraft Structural Design (Including Loads); Structural Static Analysis.

* Associate Professor, Department of Mechanical Engineering.
† Senior Research Associate, Department of Mechanical Engineering.

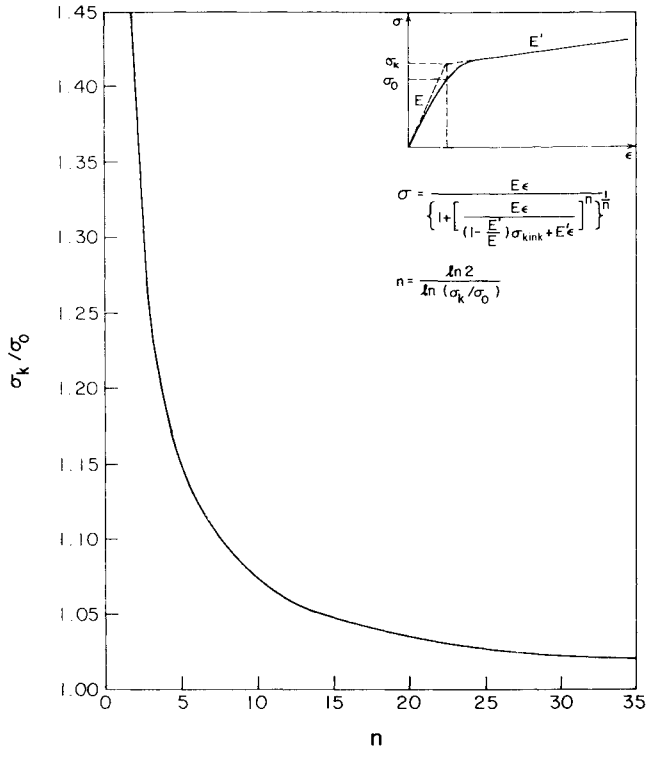

Fig. 1 Variation of the stress power n.

material stiffness has to be taken into account in the computations. In order to overcome this difficulty, piecewise linearity has been assumed in dealing with plasticity analysis, so that the well established linear theory of elasticity can be used. This type of treatment has been described in detail in several publications, for example in Ref. 2.

Literature review indicated that almost all the published results from the incremental finite element theories use predetermined piecewise linear approximations of stress-strain curves. Such an approach necessitates the use of the concept of the initial yield functions and relies on the elastic behavior of the material up to this initial yield surface. Since in practice such a yield surface is in fact determined from measuring a fixed percentage of plastic deformation (notedly 0.2% offset of strain for ductile materials), complications arise when the state of some parts of the structure is very near the elasto-plastic transition. It is necessary to make an accurate estimate and subsequent iterations of the next load increment so that the state of stresses in these parts will not deviate from its stress-strain relation. One of such techniques is to use the "mean stiffness" in the analysis.[3] A better and simpler solution to this problem is to make use of continuous approximations of the measured stress-strain behavior such as suggested by Richard and Blacklock.[4] By introducing such continuous stress-strain relations, the critical elastic-plastic transition of the element material becomes immaterial and thus allows continuous computation of the element stress with reasonable load increments.

The continuous family of constitutive relations proposed in Ref. 4 are for the use in an approximate inelastic method of finite element structural analysis (not based on the incremental method). However, a significant shortcoming of their model is that its application is limited to the nonhardening ideally plastic materials, which is not practical as most engineering materials at large plastic strain usually exhibit linear work hardening. Further, for many practical applications, the strain rate and temperature dependent "true stress" vs "true strain" curves should be used in place of the usual "engineering stress" vs "engineering strain" curves. Existing data indicate that "true stress" vs "true strain" curves for most materials exhibit a shape very similar to bilinear stress-strain curves. Modifications to the existing model is thus necessary to accommodate this important feature.

The proposed new constitutive stress-strain relation for the general material behavior takes the form:

$$\bar{\sigma} = \frac{E\bar{\varepsilon}}{\left\{1+\left[\frac{E\bar{\varepsilon}}{(1-E'/E)\bar{\sigma}_K+E'\bar{\varepsilon}}\right]^n\right\}^{1/n}} \tag{1}$$

where $\bar{\sigma}, \bar{\varepsilon}$ = effective stress and strain, respectively; E, E' = moduli of elasticity and plasticity, respectively; $\bar{\sigma}_K$ = stress level at the intersection (kink) of the elasto-plastic curve as shown in Fig. 1.

The stress power n in Eq. (1) may be estimated either by the following expression:

$$n = \ln 2/\ln(\sigma_K/\sigma_0) \tag{2}$$

or from the curve shown in Fig. 1.

The shape of the stress vs strain curves with different values of n has been shown in Fig. 2. It is obvious that the lower the values of n the more smooth the curves, such as for highly ductile materials. For most materials, the transition from the elasticity

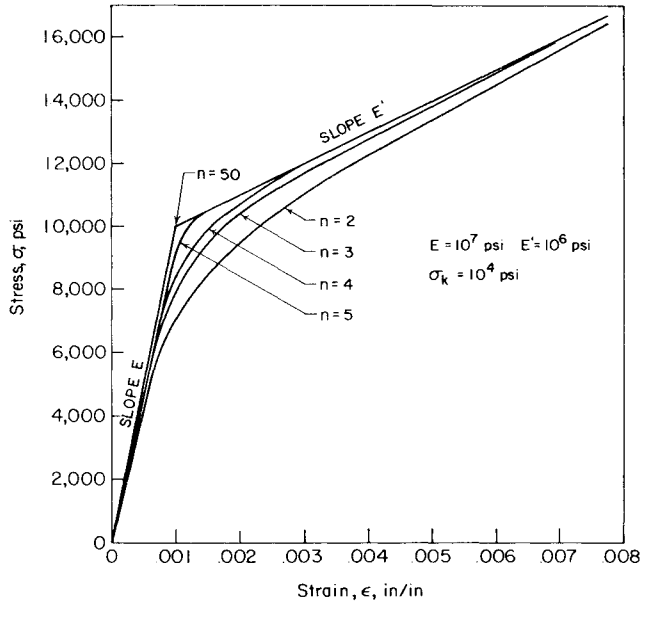

Fig. 2 Stress vs strain curves with different values of n.

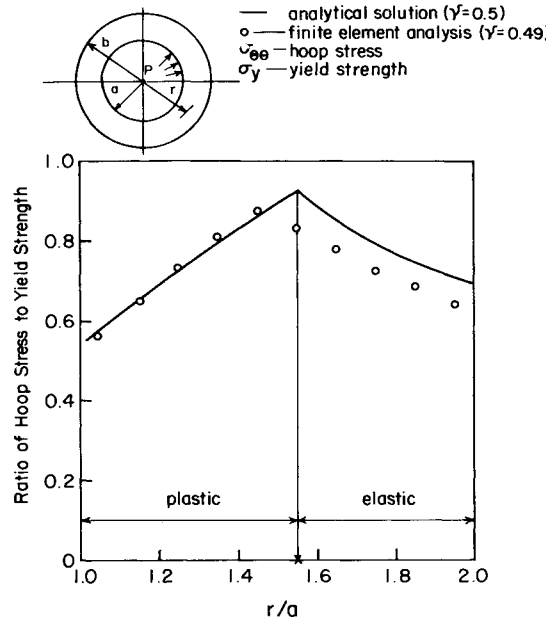

Fig. 3 Distribution of hoop stress in a thick wall cylinder.

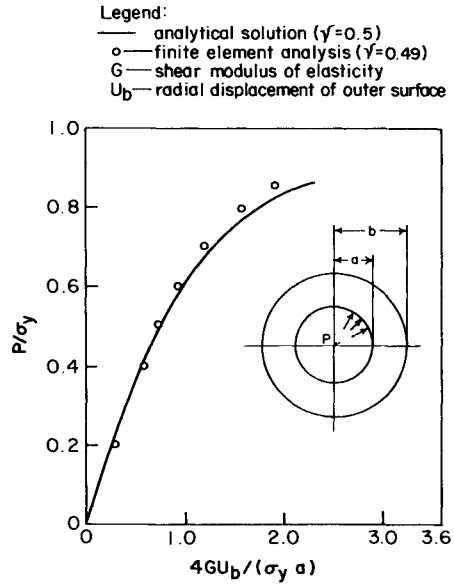

Fig. 4 Variation of radial displacement of a thick wall cylinder.

to plasticity is rather abrupt; high values of η should be used. It is easy to visualize the case $E' = 0$ implies the ideally plastic material and Eq. (1) gives identical results as the model described in Ref. 4.

A computer program was developed by the authors to handle the elastic-plastic stress analysis for the axisymmetric structures by the finite element variational technique. The elastic-plastic stiffness matrix derived by Yamada et al.[5] and the constitutive relation of Eq. (1) served as the basis for such programing. The analytical solution for a thick wall cylinder of linear work hardening material subjected to internal pressure loading given in Ref. 6 was used to check the results obtained by the finite element analysis. The stress-strain relation of the material is assumed to be depicted by the curves shown in Fig. 2 with stress power $n = 50$. The comparison of the two solutions is shown in Figs. 3 and 4. It may be visualized that the agreement of the results is excellent in plastic range whereas discrepancies in the tangential stress distribution occur in the elastic part of the solution. These discrepancies are mainly attributed to the assumption made in the analytical solution that the cylinder material is incompressible. The Poisson's ratio was assumed to be 0.5 throughout the elastic-plastic analysis. This value of Poisson's ratio causes numerical instability in calculating the elastic stiffness matrix in the finite element computations. A lower value of 0.49 had to be used. This number was close to that used in the analytical solution but was still too close to 0.5. A somewhat inaccurate result was thus obtained in the elastic portion of the finite element analysis.

The constitutive equation suggested in Eq. (1) has been proven to be versatile and practical for handling general elastic-plastic stress analysis of solid structures. The tedious iterations for estimating the proper load increments for the structural elements near the elasto-plastic transition region can be avoided by using this simple relation.

References

[1] Hsu, T. R., Bertels, A. W. M., Arya, B., and Banerjee, S., "Application of the Finite Element to the Non-linear Analysis of Nuclear Reactor Fuel Behaviour," *Proceedings of the First International Conference on Computational Methods in Non-linear Mechanics*, Univ. of Austin, Austin, Texas, Sept. 1974.

[2] Zienkiewicz, O. and Cheung, Y., *The Finite Element Method in Sustructural and Continuum Mechanics*, McGraw-Hill, New York, 1967.

[3] Marcal, P. V., "A Stiffness Method for Elastic-Plastic Problems," *International Journal of Mechanical Sciences*, Vol. 7, 1965, pp. 229–238.

[4] Richard, R. M. and Blacklock, J. R., "Finite Element Analysis of Inelastic Structure," *AIAA Journal*, Vol. 7, No. 3, March 1969, pp. 432–438.

[5] Yamada, Y., Yoshimura, N., and Sakurai, T., "Plastic Stress-Strain Matrix and Its Application for the Solution of Elastic-Plastic Problem by the Finite Element Method," *International Journal of Mechanical Sciences*, Vol. 10, 1968, pp. 343–354.

[6] D'Isa, F. A., *Mechanics of Metals*, Addison-Wesley, Reading, Mass., 1968, p. 211.

Technical Comments

Comment on "Neighboring Extremals for Optimal Control Problems"

LINCOLN J. WOOD*
California Institute of Technology, Pasadena, Calif.

IN a recent paper, Hymas, Cavin, and Colunga[1] discussed the extension of earlier work on neighboring optimal control for problems without path constraints to problems with a state variable inequality constraint. The purposes of this Comment are to point out a number of errors in their paper, to mention that similar work in this area has been done by Speyer,[2] and to discuss several consequences of the new first-order necessary conditions of Jacobson, Lele, and Speyer[3] which the authors have not considered.

A control constraint on a state constrained arc may be obtained by differentiating the state constraint with respect to time until the control appears explicitly. If q such differentiations are required, the state constraint is said to have order q. Two techniques for handling state constrained problems by means of variational calculus are discussed by Speyer.[2] One involves adjoining the state constraint directly to the Hamiltonian with an undetermined multiplier; the other involves adjoining the control constraint to the Hamiltonian along the constrained arc, and also adjoining a q-dimensional set of entry (or exit) constraints to the performance index. Hymas et al., follow a modified form of the latter approach, using the control constraint to eliminate the control (assumed scalar) immediately, rather than adjoining the control constraint to the Hamiltonian. Hence, their Hamiltonian is defined differently than in Ref. 2. Using Hymas' approach

$$\lambda^T = -H_x + H_u Z_u^{-1} Z_x$$

with $H_u \neq 0$, in general, on constrained arcs.

Speyer generalizes the backward sweep method of McReynolds[4] for solving two-point boundary-value problems to the state constrained case, and states jump conditions for the backward sweep matrices (with a few minor mistakes). Similar jump conditions for problems with interior point constraints are stated in greater detail in Ref. 5. Hymas et al. also describe a backward sweep, which includes a number of errors, as described below. All equations cited by number are equations in Ref. 1.

Received September 25, 1973; revision received March 7, 1974.
Index category: Navigation, Control, and Guidance Theory.
* Bechtel Instructor in Engineering. Member AIAA.